Journal of Engineering Mathematics **38:** 101–118, 2000.

The effect of spatial inhomogeneity in thermal conductivity on the formation of hot-spots

A. ANDONOWATI[1] and DANIEL CHANDRA[2]
[1]*Faculty of Mathematical Sciences, University of Twente, P.O. Box 217, 7500 AE Enschede, The Netherlands. e-mail: aan@math.utwente.nl* and
Department of Mathematics, Institut Teknologi Bandung, Jl. Ganesha 10 Bandung, Indonesia
[2]*Department of Mathematics and Computing Science, Eindhoven University of Technology, P.O. Box 513, 5600 MB Eindhoven, The Netherlands. e-mail: danielc@win.tue.nl* (address for correspondence)

Received 12 November 1998; accepted in revised form 2 July 1999

Abstract. The steady-state microwave heating of a unit slab consisting of three layers of materials with different thermal conductivities is examined. The governing equations are a damped wave equation derived from Maxwell's equations and a heat-force equation for the temperature. As the primary concern is to investigate the dependence of the steady-state on the thermal-conductivity parameter, a simplifying assumption is made, namely that the electrical conductivity is temperature-independent. Under this assumption, the damped wave equation governing the electric field may be solved separately. An eigenfunction expansion for the problem based on the Galerkin method is described and a fundamental-mode approximation is presented. If this approximation is applied to a unit slab composed of three layers with different thermal conductivities, the hot-spot formation can be addressed and a global steady-state solution is found for the whole domain. Numerical results for some different cases of the three-layer combinations are interpreted to gain some insight in parameter dependence and the position of the low-thermal-conductivity inner layer related to hot-spot formation.

Key words: microwave heating, hot-spot, spatial inhomogeneity, thermal conductivity, fundamental-mode approximation.

1. Introduction

In recent years there has been a growing interest in the use of microwave radiation for industrial processing such as drying, melting, smelting, and sintering. This heating technique is proved to have some advantages over the use of a conventional oven. In the sintering of ceramics, for example, the use of a conventional oven for prolonged periods of time is required to achieve high equilibrium temperatures in processes that are controlled by thermal conductivity [1]. Generating heat internally by means of microwave energy can significantly reduce the time as required in conventional sintering [2–5]. The widespread industrial applications of microwave heating have also created a number of problems. For most of these problems there is the formation of a hot-spot, which is a small region of very high temperature relative to the surroundings. Such a phenomenon can either be desirable, such as in metal melting, or undesirable, such as in ceramic sintering.

In general, the microwave heating of a material involves a coupling of electromagnetic and thermal phenomena. These phenomena can be expressed mathematically as a system consisting of a damped wave equation derived from Maxwell's equations governing the propagation of the microwave radiation and a forced heat equation governing the resultant of heat flow. The forcing term in the last equation is proportional to the square amplitude of the microwave field.

General analysis of this kind of microwave heating of a material is not easy. Until recently, the mathematical analysis of the problem was divided into two main streams [6]. First, under assumption that the properties of the heated material are slowly varying with temperature, the effects of the electromagnetic field are of interest. In this case, perturbation solutions are found for both the electric field and the temperature. Such studies have been carried out by a number of authors such as Kriegsmann *et al.* [1], Kriegsmann [7], Picombe and Smyth [8], Smyth [9] and Marchant and Picombe [10]. When the thermal aspects are isolated, a simplifying assumption can be made, namely that the microwave radiation has a constant amplitude, [11–13], leading to a single heat-force equation for the temperature $\theta_t = \nu\nabla^2\theta + f(\theta)$. Here, $f(\theta)$ is the temperature-dependent rate of energy absorption by the material.

Using the second approach, Colleman [11] investigated hot-spot formation for different functions describing the temperature-dependent reaction rate $f(\theta)$. In the case of an Arrhenius dependency of the form $f(\theta) = \delta\,\mathrm{e}^{-\gamma/\theta}$, he found numerically that, for sufficiently small ν, θ becomes large in finite time, signifying the formation of a hot-spot. For a dependency of the form $f(\theta) = \delta\,\mathrm{e}^{-\gamma/\theta}$, Hill and Smyth [13] found steady-state solutions in planar and cylindrical geometries with constant ν and constant temperature on the boundary of the body. For a quadratic dependence on temperature of the reaction rate $f(\theta)$ and a connective heat-lost boundary condition, for a cylindrical body, Roussy *et al.* [13] found numerically an approximate criterion for a hot-spot to form. It is noted that, based on an analysis of the experimental data collected for various materials, Hill and Jennings [14] found that linear, quadratic and exponential temperature dependencies of the reaction rate $f(\theta)$ are valid for many materials.

Recently Pelesko and Kriegsmann [15] studied the microwave heating of a one-dimensional ceramic laminate composed of three layers of two different types of material (identical outer layers and an inside layer). These two materials have widely disparate effective electrical conductivities. The two governing equations considered were the damped wave equation governing the propagation of the microwave radiation and the forced-heat equation governing the resultant of heat flow. An asymptotic theory was set up based on the assumption that the ratio of the two conductivities is small. This approach yields simplified equations which were then analyzed numerically. Marchant and Liu in [16] used a Galerkin method to find the steady-state microwave heating of a one-dimensional finite slab with electrical conductivity and thermal absorptivity governed by the Arrhenius function which, in that paper, was approximated by a rational cubic function. The boundary conditions took account of both connective and radiative heat losses. For small thermal absorptivity, approximate analytical solutions were found for the steady-state temperature as well as the electric-field amplitude. Multi-valued steady-state temperatures were found for the S-shaped curve of temperature-versus-power relationship. The thermal runaway was described as when the temperature jumps from the lower to the upper branch of the curve.

The present paper is concerned with a finite slab consisting three layers. Contrary to the three layers in the work of Palesko and Kriegsmann [15] where the electrical conductivity is of interest, here we assume that the layers have different thermal conductivities (thermal diffusivities). An Arrhenius-type of temperature dependency of the reaction rate of the form $f(\theta) = \mathrm{e}^{\alpha\theta/(\alpha+\theta)}$ for some $\alpha > 0$ is used. Using the approach in [17] that is, assuming a temperature independent of the electrical conductivity of the material and microwave speed, we may solve the damped wave equation separately which leads to a single forced heat equation governing the resulting heat flow. The forcing term in the last equation is proportional to the spatially dependent squared amplitude of the microwave field. The technique exploited is a one-term Galerkian approximation. It was shown in [18] and [19] that such an approximation makes sense to obtain the salient features of the solution. In this paper, we address the hot-spot formation by finding a global steady-state solution for the whole domain of different thermal conductivities. Although the paper is concerned with hot-spot formation, the approach may be applied to a three-layer configuration of a finite slab. The novelty of this approach lies in its simplicity.

In the next section, we present the governing equations for the microwave heating of a material which consists of a damped wave equation that is derived from Maxwell's equations and a heat-force equation for the temperature. As our primary concern is to investigate the influence of the spatial dependence of the thermal conductivity of the material, the simplifying assumption is made that the electrical conductivity is temperature-independent. Under this assumption, the equation governing the electrical field may be solved separately. In Section 3 some preliminary results and an eigenfunction expansion based on a Galerkin approximation are presented. For some geometries (unit sphere, finite cylinder, and rectangular block) with Dirichlet boundary conditions, it has been shown, numerically ([18, 20]), that the fundamental mode is dominant. The critical parameters obtained by using this single mode approximate the critical parameters of the solution. For this reason, we focus on this fundamental mode. The formulation of the problem for a unit slab consisting three layers of different thermal conductivities is presented in Section 4. An analysis based on the one-term Galerkin approximation is presented in the same section. In Section 5, we present some numerical results for some different cases of the three-layer combinations. In the last section concluding remarks are given.

2. Governing equations

The equations governing the microwave heating of a material are the damped wave equation derived from Maxwell's equations governing the propagation of the microwave radiation and the forced heat equation governing the flow of heat [17],

$$E_{tt} + \sigma(\theta)E_t = c^2\nabla^2 E, \tag{1}$$

$$\theta_t = \nabla.(k(\theta)\nabla\theta) + \delta|E|^2 f(\theta). \tag{2}$$

Here, E and θ are the electric field associated with the microwave heating radiation and the temperature, respectively. The temperature-dependent parameter σ is the electrical conductivity of the material and c is the microwave speed. Further, $|E|$ is the amplitude of the electric field, $k(\theta)$ is thermal conductivity of the material with the properties $k(\theta) > 0, k'(\theta) > 0$, while $f(\theta)$ is the rate of the microwave energy absorption by the material with properties $f(\theta) > 0$, $f'(\theta) > 0$. Here, we take $f(\theta)$ to be of Arrhenius type of the form $f(\theta) = \mathrm{e}^{\alpha\theta/(\alpha+\theta)}$ for some $\alpha > 0$. The damped wave equation (1) may be derived from the Maxwell's equations under the assumption that σ is small and that the microwave speed c is temperature-independent.

It is difficult to solve the set of Equations (1) and (2) with temperature-dependent σ. In this work we make the simplifying assumption that σ is constant. Although this creates an unphysical temperature variation in σ, our primary concern is to investigate the spatial dependence of the thermal conductivity of the material $k(\theta)$. Under this assumption, in the one-dimensional domain, Equations (1) and (2) become

$$E_{tt} + \sigma E_t = c^2 E_{xx}, \tag{3}$$

$$\theta_t = \frac{\partial}{\partial x}\left(k(\theta)\frac{\partial}{\partial x}\theta\right) + \delta|E|^2 f(\theta). \tag{4}$$

The damped wave Equation (3) has a travelling-wave solution of the form

$$E = \mathrm{e}^{-k_1 x}\,\mathrm{e}^{\mathrm{i}(kx-\omega t)}, \tag{5}$$

where

$$k^2 = \frac{\omega^2}{2c^2}\left[1 + \left(1 + \frac{\sigma^2}{\omega^2}\right)^{1/2}\right]$$

and

$$k_1^2 = \frac{\omega^2}{2c^2}\left[-1 + \left(1 + \frac{\sigma^2}{\omega^2}\right)^{1/2}\right].$$

Using the above assumption, we can write the forced heat equation (2) in the form

$$\theta_t = \frac{\partial}{\partial x}\left[k(\theta)\frac{\partial}{\partial x}\theta\right] + \delta R(x) f(\theta), \tag{6}$$

where $R(x) = |E|^2$ and the expression for E is of the form (5). Note that, for $k(\theta) = 1$ and $R(x) = 1$, Equation (6) features prominently in combustion theory and has been studied by many authors such as in [21, Chapters 2–4], [22–24] and many others.

In the above model the conductivity parameter μ, which measures the magnitude of thermal conductivity of the material, is constant throughout the medium D. In this work, however, we intend to investigate the effect of inhomogeneity of μ on the formation of a hot-spot, which is a small region in the heated medium where the temperature is much higher than elsewhere. For the domain D we take a unit slab [0, 1] and the conductivity is given by $k(\theta) = \mu(x)\,\mathrm{e}^{\gamma x}$, where $\mu(x)$ is a function of the spatial variable x, namely

$$k(\theta) = \begin{cases} \mu_1\,\mathrm{e}^{\gamma\theta} & \text{if } 0 \leqslant x < x_0, \\ \mu_2\,\mathrm{e}^{\gamma\theta} & \text{if } x_0 \leqslant x \leqslant x_0 + \varepsilon, \\ \mu_3\,\mathrm{e}^{\gamma\theta} & \text{if } x_0 + \varepsilon < x \leqslant 1, \end{cases}$$

where $\mu_2 < \mu_1$ and $\mu_2 < \mu_3$. Here, we address hot-spot formation by finding a global steady-state solution for the whole region [0, 1] in which this formation appears, which is in the region $[x_0, x_0 + \varepsilon]$.

3. Analysis of the reduced equation

We consider a model

$$\frac{\partial\theta}{\partial t} = \nabla\cdot(k(\theta)\nabla\theta) + \delta R(\mathbf{x}) f(\theta). \tag{7}$$

Using the transformation

$$v = \int_0^\theta k(s)\,\mathrm{d}s, \tag{8}$$

we may write Equation (7) as follows

$$\frac{\partial v}{\partial t} = K(v)\{\nabla^2 v + \delta E(\mathbf{x})F(v)\},$$

where $K(v) = k(\theta(v))$ and $F(v) = f(\theta(v))$. Since $u(\theta)$ is monotonically increasing, we observe that both $K(u)$ and $F(u)$ have the same features as $k(\theta)$ and $f(\theta)$, respectively. We can remove the function $K(v)$ by letting τ to be such that $\mathrm{d}\tau/\mathrm{d}t = K(v(\mathbf{x},t))$ and $u(\mathbf{x},\tau) = v(\mathbf{x},t)$ giving

$$\frac{\partial u}{\partial \tau} = \nabla^2 u + \delta R(\mathbf{x})F(u).$$

3.1. Behaviour of solutions

We will now study the behaviour of the solution of the equation

$$\frac{\partial u}{\partial t} = \nabla^2 u + \delta R(\mathbf{x})F(u), \tag{9}$$

subject the initial and Dirichlet boundary conditions

$$u(\mathbf{x},0) = H(\mathbf{x}), \qquad u(\mathbf{x},t) = 0 \quad \text{on } \partial D. \tag{10}$$

From the transformation (8) the function F in (9) can be written in the form

$$F(u) = f(\theta(u)) = \exp\left\{\frac{\dfrac{\alpha}{\gamma}\log(1+\gamma u/\mu)}{\alpha + \dfrac{1}{\gamma}\log(1+\gamma u/\mu)}\right\}.$$

For completeness the following results are summarized from [18]. First, we consider the following boundary-value problem

$$\frac{\partial U}{\partial t} = \nabla^2 U + \delta R(\mathbf{x})F(m), \tag{11}$$

$$U(\mathbf{x},0) = H(\mathbf{x}), \qquad U(\mathbf{x},t) = 0 \quad \text{on } \partial D. \tag{12}$$

for some parameter $m \leqslant 0$. Let $\bar{u}$ and $\bar{U}$ denote the steady-state solution of (9), (10) and (11), (12), respectively. If $m = \max_{\mathbf{x}}\bar{u}(\mathbf{x})$, then, by the minimum principle, we can show that $\bar{U}(\mathbf{x},m) \geqslant m$.

Let φ_n and λ_n be the normalized eigenfunctions and eigenvalues of the boundary-value problem

$$\nabla^2\varphi_n = -\lambda_n\varphi_n, \qquad \varphi_n = 0 \quad \text{on } \partial D,$$

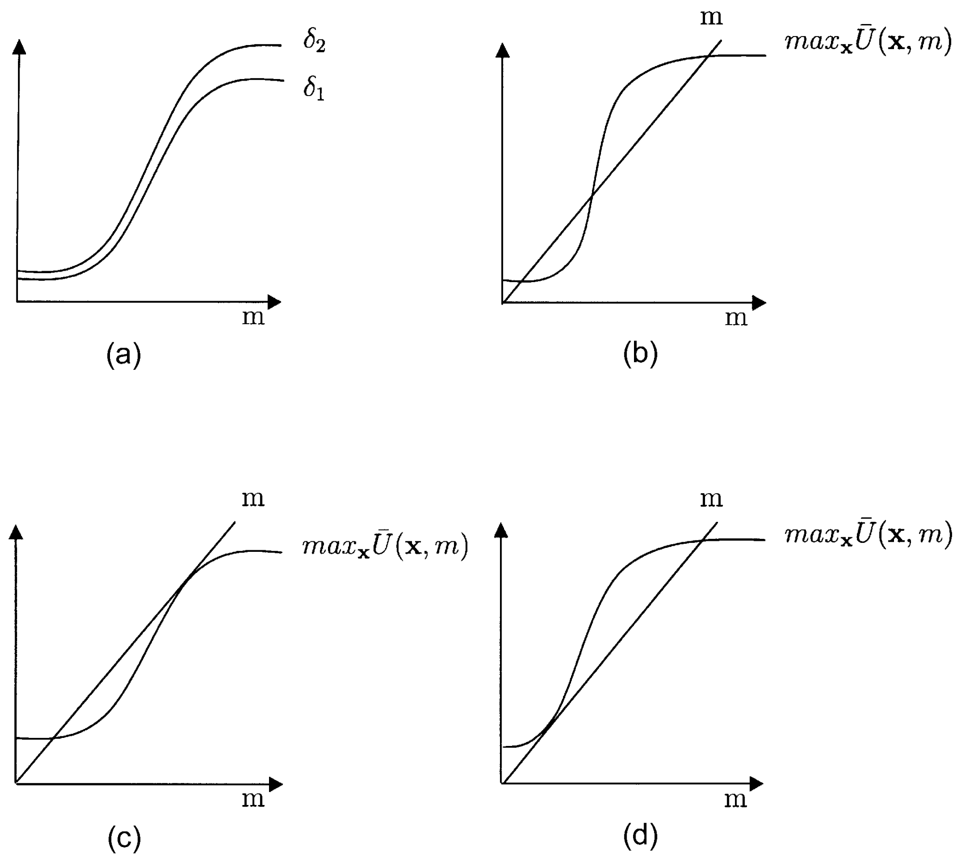

Figure 1. (a) $\max_{\mathbf{x}} \bar{U}(\mathbf{x}, m)$ *vs.* m for different δ, $\delta_1 < \delta_2$; (b) Intersections of $\max_{\mathbf{x}} \bar{U}(\mathbf{x}, m)$ *vs.* m and the line m; (c) $\max_{\mathbf{x}} \bar{U}(\mathbf{x}, m)$ *vs.* m for $\delta = \delta_{U\mathrm{cr}}$; (d) $\max_{\mathbf{x}} \bar{U}(\mathbf{x}, m)$ *vs.* m for $\delta = \delta^{U\mathrm{cr}}$.

where $\lambda_1 < \lambda_2 \leqslant \lambda_3 \leqslant \cdots$. The steady-state solution of (11), (12) may be written in the form $\bar{U}(\mathbf{x}, m) = \delta F(m)\ \Sigma_i \frac{B_i}{\lambda_i}\ \varphi_i(\mathbf{x})$, where $B_i = \int_D R(x)\ \varphi_i(\mathbf{x})\, \mathrm{d}\mathbf{x}$. If we write $M = \max_{\mathbf{x}} \Sigma_i \frac{B_i}{\lambda_i} \varphi_i(\mathbf{x})$ then $\max_{\mathbf{x}} \bar{U}\ (\mathbf{x}, m) = \delta M F(m)$. Taking $\mu = 1$, we note that

$$F'(m) = \frac{(\alpha\gamma)^2 F(m)}{[1 + \gamma m][\alpha\gamma + \log(1 + \gamma m)]},$$

while

$$F''(m) = \frac{\alpha^2 \gamma^3 G(\alpha, \gamma, m) F(m)}{[1 + \gamma m]^2 [\alpha\gamma + \log(1 + \gamma m)]^3},$$

where

$$G(\alpha, \gamma, m) = \alpha\gamma(\alpha - 2 - \alpha\gamma) - \log(1 + \gamma m)[2 + 2\gamma\alpha + \log(1 + \gamma m)],$$

giving $F'(m) > 0$ for $m \geqslant 0$ and, if $\alpha(1 - \gamma) \leqslant 2$, then $F''(m) < 0$, for $m > 0$ and so the graph of $F(m)$ *vs.* m intersects the line m at one and only one point for any value of δ. For $\mu = 1$, a necessary condition such that the graph of $F(m)$ *vs.* m is in the form of an S-shaped curve is that $\alpha(1 - \gamma) > 2$. This analysis will still hold later for the one-term Galerkin approximation, provided that the first mode $\varphi_1(\mathbf{x})$ is nonnegative throughout the region D. For some values of α and γ such that the graph $F(m)$ *vs.* m has an S-shaped curve, Figure 1(a) shows the graph of $\max_{\mathbf{x}}\bar{U}(\mathbf{x}, m)$ *vs.* m for different values of δ.

When the graph of $F(m)$ *vs.* m has an S-shaped curve, for which is necessary that $\alpha(1-\gamma) > 2$, using the maximum principle, we can show (see [18]) that

(1) If δ is such that $\max_{\mathbf{x}}\bar{U}(\mathbf{x}, m) - m = 0$ has a single root, say m_0, then $\max_{\mathbf{x}}\bar{u}(\mathbf{x}) \leqslant m_0$.
(2) If δ is such that $\max_{\mathbf{x}}\bar{U}(\mathbf{x}, m) - m = 0$ has three roots, say m_1, m_2, m_3, where $m_1 < m_2 < m_3$, [see Figure 1(b)], then $0 \leqslant \max_{\mathbf{x}}\bar{u}(\mathbf{x}) \leqslant m_1$ or $m_2 \leqslant \max_{\mathbf{x}}\bar{u}(\mathbf{x}) \leqslant m_3$. Here we note that m_1 is $O(1)$ while m_3 is $O(\mathrm{e}^{\alpha})$.

Let $\delta^{U_{\mathrm{cr}}}$ and $\delta_{U_{\mathrm{cr}}}$ be the largest and the smallest value of δ such that the line m is tangent to the lower and upper portion of the graph $\max_{\mathbf{x}}\bar{U}(\mathbf{x}, m)$ *vs* m, respectively [see Figures 1(c) and 1(d)]. Let δ be such that $\delta^{U_{\mathrm{cr}}} < \delta < \delta_{U_{\mathrm{cr}}}$. Then, for these values of δ, $\max_{\mathbf{x}}\bar{U}(\mathbf{x}, m) - m = 0$ has three roots. Since $\bar{U}(\mathbf{x}, m)$ is an upper solution of $\bar{u}(\mathbf{x})$ then, if $H(\mathbf{x}) = 0$, $u(\mathbf{x}, t)$ will be $O(1)$ for all t. This value $\delta^{U_{\mathrm{cr}}}$ is a lower bound of the critical value δ^{cr}, where the steady-state solution $\bar{u}$ undergoes a rapid transition from $O(1)$ to $O(\mathrm{e}^{\alpha})$.

3.2. Fundamental-mode approximation

Let us return to the boundary-value problem (9), (10). Adopting the following approximation procedure, which can be attributed to Galerkin, let us write

$$s_N(\mathbf{x}, t) = \Sigma_{i=1}^{i=N} A_i^{(N)}(t)\varphi_i(\mathbf{x}),$$

where $A_i^{(N)}(t)$ is the solution of the integral equation

$$\frac{\mathrm{d}A_i^{(N)}}{\mathrm{d}t} = -\lambda_i A_i^{(N)} + \delta \int_D R(\mathbf{x}) F(\Sigma_{i=1}^{i=N} A_i^{(N)} \varphi_i(\mathbf{x}))\varphi_i(\mathbf{x})\, \mathrm{d}v(\mathbf{x}),$$

for $1 \leqslant i \leqslant N$. The above equations constitute N integral equations with N unknowns.

From the behaviour of the solution as studied above and assuming that the first eigenfunction $\varphi_1(\mathbf{x})$ is nonnegative, we conclude that it makes sense to adopt a fundamental-mode approximation, $s_1(\mathbf{x}, t) = A(t)\varphi_1(\mathbf{x})$. This $A(t)$ (may be thought of as being similar to $\max_{\mathbf{x}} u(\mathbf{x}, t)$) is obtained from the integral equation

$$\frac{\mathrm{d}A}{\mathrm{d}t} = -\lambda_1 A + \delta \int_D R(\mathbf{x}) F(A\varphi_1(\mathbf{x}))\varphi_1(\mathbf{x})\, \mathrm{d}v(\mathbf{x}), \tag{13}$$

Let

$$I(A) = \int_D R(\mathbf{x}) F(A\varphi_1(\mathbf{x}))\varphi_1(\mathbf{x})\, \mathrm{d}v(\mathbf{x}). \tag{14}$$

The equilibrium values of A can be obtained graphically from the intersection of the straight line $\lambda_1^2 A/\delta$ *vs.* A and the curve of the graph $I(A)$ *vs* A. Similar to the result found in the previous subsection, it is not difficult to see that for $\mu = 1$ a necessary condition for the graph $I(A)$ *vs.* A to be S-shaped is

$$\alpha(1-\gamma) > 2.$$

For $\alpha(1-\gamma) \leqslant 2$ there is only one possible steady-state solution for A. In combustion this phenomenon is often called 'loss of criticality' which occurs for the critical values of α and and γ such that $\alpha(1-\gamma) \leqslant 2$. Lacey and Wake [22] showed that, for a simpler equation $\nabla \cdot (\mathrm{e}^{\gamma\theta}\nabla\theta) + \delta\,\mathrm{e}^{\theta} = 0$, the solution does not exhibit a critical phenomenon when $\gamma \geqslant 1$. Tam ([24]) showed that for a sphere of unit radius with $\alpha = 100$, loss of criticality occurs when $\gamma = 0{\cdot}9$. From the simple analysis given above for $\alpha = 100$, loss of criticality occurs when $\gamma = 0{\cdot}95$.

When the graph $I(A)$ *vs.* A has an S-shape, there are two critical parameters of δ, say δ^{cr} and δ_{cr}. The critical value δ^{cr}, where the steady state of (13) is $O(\mathrm{e}^{\alpha})$ for $\delta > \delta^{\mathrm{cr}}$, is obtained when the straight line $\lambda_1^2 A/\delta$ *vs.* A is tangent to the lower portion of the S-shaped curve. On the other-hand, the critical value δ_{cr}, where the steady state of (13) is $O(1)$ for $\delta < \delta_{\mathrm{cr}}$, is obtained when the straight line $\lambda_1^2 A/\delta$ *vs.* A is tangent to the upper portion of the S-shaped curve. For δ, $\delta_{\mathrm{cr}} < \delta < \delta^{\mathrm{cr}}$, for some critical values δ_{cr} and δ^{cr}, depending on the initial condition $A(0) = C_1$, there are three possible steady-state solutions for Equation (13), say A_1, A_2, and A_3, where $A_1 < A_2 < A_3$ and A_1 is of $O(1)$, A_3 is of $O(\mathrm{e}^{\alpha})$. We note that the middle solution A_2 is unstable, whereas, the other two are stable.

For a few different configurations of the medium, *viz.* a unit sphere, a finite cylinder and a rectangular block, it is shown in [18, 20], that it is not only the first mode which is dominant, but also the critical values δ_{cr} and δ^{cr} obtained by using a single mode, close to the critical values δ of u.

3.3. Steady-state solution for a unit slab geometry

To illustrate the method described above, let us consider a unit-slab geometry [0, 1]. For this slab, we have the first eigenvalue $\lambda_1 = \pi^2$ corresponding to the normalized eigenfunction $\varphi_1 = \sqrt{1/2\pi}\,\sin(\pi x)$. Taking an exponential function of $R(x) = |E|^2$, with $k = 1$ in (5), we may obtain the steady-state solutions A from

$$\frac{\lambda_1}{\delta} A = \int_D R(\mathbf{x}) F(A\varphi_1(\mathbf{x}))\varphi_1(\mathbf{x})\,\mathrm{d}v(\mathbf{x}).$$

The critical parameter δ^{cr} can be approximated as follows. Let A_1 be the smallest A satisfying $I(A_1) = \lambda_1 A_1/\delta^{\mathrm{cr}}$ then

$$\frac{\mathrm{d}}{\mathrm{d}A}\left[I(A) - \frac{\lambda_1 A}{\delta^{\mathrm{cr}}}\right]_{A=A_1} = 0.$$

Thus, we can calculate δ^{cr} by first obtaining the value of A_1 from

$$I(A_1) - A_1 I'(A_1) = 0$$

and then

$$\delta_{\mathrm{cr}} = \frac{\lambda_1 A}{I(A_1)}.$$

For $\alpha = 10$, $\mu = 1$, $\gamma = 0{\cdot}1$, Figure 2 shows a bifurcation diagram for the temperature θ as obtained from the inverse of the transformation (8) and the fundamental-mode approximation, that is $\theta \approx \log(1 + \gamma A\varphi_1/\mu)/\gamma$. The parameter δ can be seen as the magnitude of the square

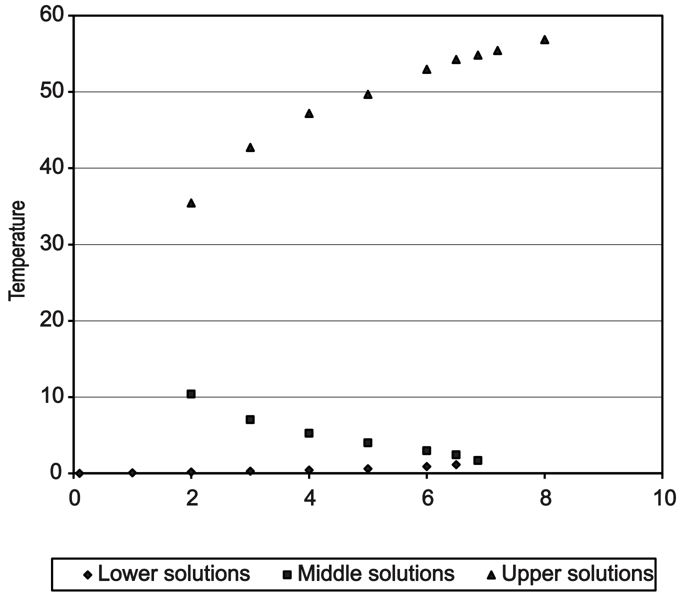

Figure 2. Bifurcation diagram of the temperature θ *vs.* δ evaluated at $x = 0{\cdot}5$.

amplitude of the electric field $R(x)$. The bifurcation diagram shows that there is a critical parameter $\delta_{\rm cr}$ such that, for $\delta < \delta_{\rm cr}$, there is only one steady-state solution θ for which the corresponding A is $O(1)$ and there is a critical parameter $\delta^{\rm cr}$ such that, for $\delta > \delta^{\rm cr}$, again there is only one steady-state solution θ, but A is $O(\mathrm{e}^{\alpha})$. The critical value $\delta^{\rm cr}$, in this computation $\delta^{cr} = 6{\cdot}869$, plays an important role in hot-spot formation. Here a slight change in the magnitude of the electric field near $\delta^{\rm cr}$ produces a substantial difference in the temperature, that is, there is a jump of the temperature from $O(1)$ to $O(\mathrm{e}^{\alpha})$. A similar result can be found in [16].

Although it is not fully justified, this simple analysis may be applied to the case of a unit slab composed of three layers of two different materials (identical outer layers and an inside layer) as was done in [15] where the two materials have widely disparate effective electrical conductivities. The magnitude of the electric field produced is a function of the electrical conductivity of the material. Thermal runaway can be experienced if the magnitude of electric field exceeds the critical value. Locally (the layers are considered as three isolated layers) thermal runaway can happen in one of the layers, but not in the others, depending on the effective electrical conductivity of the materials considered.

4. Formation of hot-spots in a three-layer finite slab

In this section we consider a unit slab composed of three layers of three different materials. As we are concerned in this work with hot-spot formation, the inside layer considered has a thermal conductivity which differs considerably from that of the outer layers. Homogeneous Dirichlet boundary conditions will be used. Although these conditions are very idealized, they have the advantage of making the investigation more managable, thus leading to a better understanding of the thermal conductivity. Future work will be done to extend this approach by including more general boundary conditions.

Let us first consider a domain D with a constant conductivity parameter μ which is constant throughout D. From the transformation (8), we obtain

$$\theta = \frac{1}{\gamma}\log\left(1 + \frac{\gamma u}{\mu}\right),$$

where the conductivity $k(\theta) = \mu\,\mathrm{e}^{\gamma\theta}$. Here $u(x,t) \approx A(t)\varphi_1(x)$, where $A(t)$ satisfies

$$\frac{\mathrm{d}A}{\mathrm{d}t} = -\lambda_1 A + \delta I(A),$$

$$A(0) = C1,$$

$$I(A) = \int_D R(x)F(A\psi_1(x))\varphi_1(x)\,\mathrm{d}x,$$

and φ_1, λ_1 are the first eigenfunction and eigenvalue of the boundary-value problem

$$\nabla^2\varphi_n = -\lambda_n\varphi_n, \quad \varphi_n = 0 \quad \text{on } \partial D.$$

Thus

$$\theta \approx \frac{1}{\gamma}\log\left(1 + \frac{\gamma A\varphi_1(x)}{\mu}\right). \tag{15}$$

It is important to note that in (15) A no longer depends on the thermal conductivity. Thus, if we consider two separate domains with conductivities $k_1 = \mu_1\,\mathrm{e}^{\gamma\theta}$ and $k_2 = \mu_2\,\mathrm{e}^{\gamma\theta}$, respectively, where $\mu_1 > \mu_2$, it is clear that the domain with with the lower conductivity μ reaches a higher temperature, independently of the value of γ. This simple analysis suggests that nonhomogeneity of thermal conductivity may contribute to the formation of hot-spots.

4.1. Formulation of the Problem

Let us consider a unit slab [0, 1] composed of three layers having thermal conductivity $k(\theta)$ expressed in the form

$$k(\theta) = \begin{cases} \mu_1\,\mathrm{e}^{\gamma\theta} & \text{if } 0 \leqslant x < x_0, \\ \mu_2\,\mathrm{e}^{\gamma\theta} & \text{if } x_0 \leqslant x \leqslant x_0 + \varepsilon, \\ \mu_3\,\mathrm{e}^{\gamma\theta} & \text{if } x_0 + \varepsilon < x \leqslant 1. \end{cases}$$

We formulate the problem by dividing the interval [0, 1] into three parts, that is $[0, x_0]$, $[x_0, x_0 + \varepsilon]$ and $[x_0 + \varepsilon, 1]$, for small ε. Let θ_1, θ_2, and θ_3 be the temperature in the intervals $[0, x_0]$, $[x_0, x_0 + \varepsilon]$ and $[x_0 + \varepsilon, 1]$, respectively. For simplification we will consider the steady-state solution only. We can obtain steady-state temperatures θ_1, θ_2 and θ_3 by solving

$$\theta_i = \frac{1}{\gamma}\log\left(1 + \frac{\gamma u_i}{\mu_i}\right), \quad i = 1, 2, 3, \tag{16}$$

where u_i is the solution of

$$\frac{\mathrm{d}^2 u_i}{\mathrm{d}x^2} + \delta R(x)F_i(u_i) = 0, \quad i = 1, 2, 3, \tag{17}$$

$$F_i(u_i) = \exp\left\{\frac{\dfrac{\alpha}{\gamma}\log\left(1+\dfrac{\gamma u_i}{\mu_i}\right)}{\alpha+\dfrac{1}{\gamma}\log\left(1+\dfrac{\gamma u_i}{\mu_i}\right)}\right\}, \quad i = 1, 2, 3.$$

Across the interfaces, the temperature θ as well as the heat flux $k(\theta)\,\mathrm{d}\theta/\mathrm{d}x$ are continuous (see [25]). Using (16) and the requirement that θ is continuous on the interfaces, that is $\theta_1(x_0) = \theta_2(x_0)$ and $\theta_2(x_0+\varepsilon) = \theta_3(x_0+\varepsilon)$, we have the conditions

$$u_1(x_0) = \mu_1 a, \qquad u_2(x_0) = \mu_2 a,$$

and

$$u_2(x_0+\varepsilon) = \mu_2 b, \qquad u_3(x_0+\varepsilon) = \mu_3 b,$$

where a and b have to be determined as part of the problem. Together with homogeneous Dirichlet boundary conditions, this continuity of the temperature yields boundary conditions for each layer

$$u_1(0) = 0, \qquad u_1(x_0) = \mu_1 a, \tag{18}$$

$$u_2(x_0) = \mu_2 a, \qquad u_2(x_0+\varepsilon) = \mu_2 b, \tag{19}$$

$$u_3(x_0+\varepsilon) = \mu_3 b, \qquad u_3(1) = 0. \tag{20}$$

The heat flux in each layer may be written as

$$k(\theta_i)\frac{\mathrm{d}\theta_i}{\mathrm{d}x} = \frac{\mathrm{e}^{\gamma\theta_i}}{1+\dfrac{\gamma u_i}{\mu_i}}\frac{\mathrm{d}u_i}{\mathrm{d}x}.$$

Noting that θ is continuous on the interfaces $x = x_0, x_0+\varepsilon$ and using the conditions for $u_i(x_0)$ and $u_i(x_0+\varepsilon)$ above, we see that the continuity of the heat flux across the interfaces may be written in the form

$$\left.\frac{\mathrm{d}u_1}{\mathrm{d}x}\right|_{x=x_0^-} = \left.\frac{\mathrm{d}u_2}{\mathrm{d}x}\right|_{x=x_0^+} \tag{21}$$

and

$$\left.\frac{\mathrm{d}u_2}{\mathrm{d}x}\right|_{x=x_0+\varepsilon^-} = \left.\frac{\mathrm{d}u_3}{\mathrm{d}x}\right|_{x=x_0+\varepsilon^+}. \tag{22}$$

In fact, the last two additional conditions may be obtained by integration of Equations (17) along the interfaces x_0 and $x_0+\varepsilon$.

4.2. Steady-state solutions

To solve the problem defined by (17), (18), (19), and (20), for all the intervals $[0, x_0]$, $[x_0, x_0+\varepsilon]$, and $[x_0+\epsilon, 1]$, we introduce the following transformations.

$$u_1 = \varphi + \mu_1 a\frac{x}{x_0}, \qquad u_2 = \psi + \mu_2\frac{(b-a)(x-x_0)}{\varepsilon} + \mu_2 a,$$

and

$$u_3 = \chi + \mu_3 b\left(1 - \frac{x - x_0 - \varepsilon}{1 - x_0 - \varepsilon}\right),$$

where φ, ψ, and χ satisfy

$$\frac{d^2\varphi}{dx^2} + \delta E(x)F_1(u_1) = 0, \qquad \varphi(0) = \varphi(x_0) = 0,$$

$$\frac{d^2\psi}{dx^2} + \delta E(x)F_2(u_2) = 0, \qquad \psi(x_0) = \psi(x_0+\varepsilon) = 0,$$

$$\frac{d^2\chi}{dx^2} + \delta E(x)F_3(u_3) = 0, \qquad \chi(x_0+\varepsilon) = \chi(1) = 0.$$

In the first interval, $[0, x_0]$, using the above transformation and the fundamental-mode approximation, we obtain $\varphi \approx A\phi_1$, where $\phi_1(x) = \sqrt{2/x_0}\sin\left(\frac{\pi}{x_0}x\right)$ is the eigenfunction corresponding to the smallest eigenvalue $\lambda_1 = \pi^2/x_0^2$ of the eigenvalue problem

$$\frac{d^2\phi}{dx^2} = -\lambda\phi, \quad \phi(0) = \phi(x_0) = 0.$$

The parameter A in this approximation satisfies

$$-A + \frac{\delta}{\lambda_1}\int_0^{x_0} E(x)F_1(u_1)\phi_1\,dx = 0, \tag{23}$$

and

$$u_1 \approx A\sqrt{\frac{2}{x_0}}\sin\left(\frac{\pi}{x_0}x\right) + \mu_1 a\frac{x}{x_0}. \tag{24}$$

For the second interval, $[x_0, x_0+\varepsilon]$, we make a transformation $\xi = x - x_0$ and so $\psi = \psi(\xi)$. Again, using the fundamental-mode approximation, we obtain $\psi_1 \approx B\vartheta_1$, where $\vartheta_1 = \sqrt{2/\varepsilon}\sin\left(\frac{\pi}{\varepsilon}\xi\right)$ is the eigenfunction corresponding to the smallest eigenvalue $\nu_1 = \pi^2/\varepsilon^2$ of the eigenvalue problem

$$\frac{d^2\vartheta}{d\xi^2} = -\nu\vartheta, \quad \vartheta(0) = \vartheta(\varepsilon) = 0.$$

Here, B satisfies

$$-B + \frac{\delta}{\nu_1}\int_{x_0}^{x_0+\varepsilon} E(x)F_2(u_2)\phi_1\,\mathrm{d}x = 0, \tag{25}$$

and

$$u_2 \approx B\sqrt{\frac{2}{\varepsilon}}\sin\left(\frac{\pi}{\varepsilon}(x-x_0)\right) + \mu_2\frac{(b-a)(x-x_0)}{\varepsilon} + \mu_2 a. \tag{26}$$

For the last interval, $[x_0+\varepsilon, 1]$, we use a transformation $\eta = x - x_0 - \varepsilon$, so that $\chi = \chi(\eta)$. Again, using the fundamental-mode approximation, we obtain $\chi \approx C\upsilon_1$, where

$$\upsilon_1 = \sqrt{\frac{2}{1-x_0-\varepsilon}}\sin\left(\frac{\pi}{1-x_0-\varepsilon}\eta\right)$$

is the eigenfunction corresponding to the smallest eigenvalue $\tau_1 = \pi^2/(1-x_0-\varepsilon)^2$ of the eigenvalue problem

$$\frac{\mathrm{d}^2\upsilon}{\mathrm{d}\eta^2} = -\tau\upsilon, \qquad \upsilon(0) = \upsilon(1-x_0-\varepsilon) = 0.$$

In this approximation C satisfies

$$-C + \frac{\delta}{\tau_1}\int_{x_0+\varepsilon}^{1} E(x)F(u_3)\phi_1\,\mathrm{d}x = 0, \tag{27}$$

and

$$u_3 \approx C\sqrt{\frac{2}{1-x_0-\varepsilon}}\sin\left(\pi\frac{x-x_0-\varepsilon}{1-x_0-\varepsilon}\right) + \mu_3 b\left(1-\frac{x-x_0-\varepsilon}{1-x_0-\varepsilon}\right). \tag{28}$$

From (23), (25) and (27), we obtain three equations and five independent variables A, B, C, a, and b. To solve them, we use the interface conditions (21) and (22) to obtain two additional equations

$$-A\left(\frac{\pi}{x_0}\right)\sqrt{\frac{2}{x_0}} + \mu_1\frac{a}{x_0} = B\left(\frac{\pi}{\varepsilon}\right)\sqrt{\frac{2}{\varepsilon}} + \mu_2\frac{b-a}{\varepsilon} \tag{29}$$

and

$$-B\left(\frac{\pi}{\varepsilon}\right)\sqrt{\frac{2}{\varepsilon}} + \mu_2\frac{b-a}{\varepsilon} = C\left(\frac{\pi}{1-x_0-\varepsilon}\right)\sqrt{\frac{2}{1-x_0-\varepsilon}} - \mu_3\frac{b}{1-x_0-\varepsilon} \tag{30}$$

Equations (29) and (30) may be written in the matrix form $\mathbf{A}[a\;b]^T = [c_1\;c_2]^T$,

$$\begin{bmatrix} \frac{\mu_1}{x_0}+\frac{\mu_2}{\varepsilon} & -\frac{\mu_2}{\varepsilon} \\ -\frac{\mu_2}{\varepsilon} & \frac{\mu_2}{\varepsilon}+\frac{\mu_3}{1-x_0-\varepsilon} \end{bmatrix}\begin{bmatrix} a \\ b \end{bmatrix} = \begin{bmatrix} A\frac{\pi}{x_0}\sqrt{\frac{2}{x_0}} + B\frac{\pi}{\varepsilon}\sqrt{\frac{2}{\varepsilon}} \\ B\frac{\pi}{\varepsilon}\sqrt{\frac{2}{\varepsilon}} + B\frac{\pi}{1-x_0-\varepsilon}\sqrt{\frac{2}{1-x_0-\varepsilon}} \end{bmatrix}. \tag{31}$$

The solution a and b (31) can be expressed in the following from

$$a = \frac{A_{22}c_1 - A_{12}c_2}{\mathrm{Det}(\mathbf{A})}, \tag{32}$$

$$b = \frac{A_{11}c_2 - A_{21}c_1}{\mathrm{Det}(\mathbf{A})}, \tag{33}$$

where Det(**A**) is the determinant of the matrix **A** in Equation (31).

Substituting (32) and (33) in (23), (25) and (27), we obtain three equations with three unknowns: A, B, and C. Using these values, we may then compute a and b from (32) and (33). Further, from (24), (26) and (28) we calculate u_1, u_2 and u_3 and finally, using

$$\theta_i = \frac{1}{\gamma}\log\left(1 + \frac{\gamma u_i}{\mu_i}\right), \quad i = 1, 2, 3,$$

we obtain the temperature θ_i, $i = 1, 2, 3$.

5. Numerical results

In the following we will present results for the smallest steady-steady solutions A, B, and C whenever there is more than one steady-state solution of (23), (25) and (27). This solution can be seen as the steady-state temperature having the initial condition equal to 0 (the normalized ambient temperature). In all computations, we have taken $\alpha = 10$, $\varepsilon = 0{\cdot}1$, $\gamma = 0{\cdot}1$, and $\delta = 1$. Based on a simplifying assumption described in Section 2, we take $R(x) = \mathrm{e}^{-|x-0{\cdot}5|}$.

First, we take $\mu_1 = \mu_3 = 1$ and $\mu_2 = 1$, 10^{-1}, 10^{-2}, 10^{-3} in Figures 3(a), 3(b), 3(c), and 3(d), respectively. The middle part of the slab is located at $x_0 = 0{\cdot}45$ in the interval [0, 1]. Figure 3(a) simply shows that the conductivity parameter μ is constant throughout the region [0, 1]. As expected, by using a fundamental-mode approximation, we find that the temperature profile in Figure 3(a) is zero on the boundaries $x = 0$ and $x = 1$ and reaches a maximum value in the middle of the slab. By taking smaller μ_2 in the region $[x_0, x_0 + \varepsilon]$, we find that the temperature in this region is higher than elsewhere. Figures 3(b), 3(c), 3(d) show that, the smaller the value of μ_2, the larger will be the discrepancy of the temperature between $[x_0, x_0 + \varepsilon]$ and the rest of the region. These figures show an interesting feature. The change in the parameter μ from 10^{-1} to 10^{-2} does not lead to a significant change in the temperature of the inner layer. However, the change of μ from the 10^{-2} to 10^{-3} results in a drastic change in the temperature of the inner layer, suggesting the existence of a critical value of μ below which thermal runaway is experienced, thus pointing to the formation of a hot-spot.

We further calculate the temperature of the middle interval of the inner layer $[x_0, x_0 + \varepsilon]$ with the same parameters as in Figure 3, but we change the values of μ from $\mu = 10^{-2}$ to $\mu = 10^{-3}$. This produces the following results

μ	0·01	0·009	0·008	0·007	0·006	0·005	0·004	0·003	0·002	0·001
θ	0·221	0·238	0·261	0·291	0·333	0·399	0·511	0·767	56·898	65·568

It shows that there is a jump in the temperature of the inner layer that occurs for values of μ in the range $0{\cdot}003 < \mu < 0{\cdot}002$. In Section 3, we made an investigation of the bifurcation

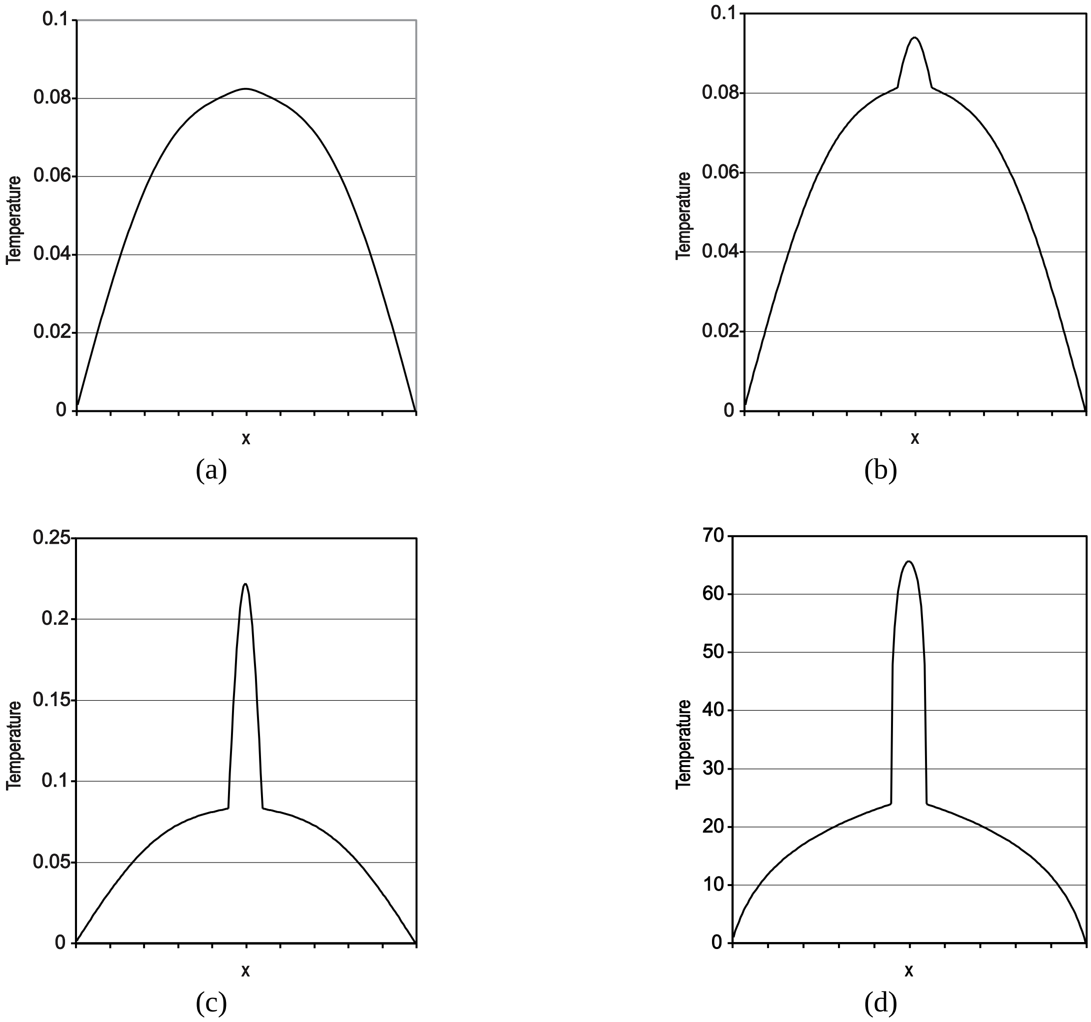

Figure 3. The steady-state temperature with a constant parameter $\gamma = 0{\cdot}1$, and for the thermal conductivity parameter $\mu_1 = \mu_3 = 1$ in outer layers while in the inner layer (a) $\mu_2 = 1$; (b) $\mu_2 = 10^{-1}$; (c) $\mu_2 = 10^{-2}$; (d) $\mu_2 = 10^{-3}$. Notice the temperature jump from the value computed for $\mu_2 = 10^{-2}$ to that computed for $\mu_2 = 10^{-3}$.

diagram of θ *vs*. the parameter δ where this δ measures the magnitude (power) of the square amplitude of the electric field. The thermal runaway is investigated through an S-shaped curve of an Arrhenius-type reaction rate of the microwave-energy absorption *vs*. temperature. There, we found a critical value δ^{cr}, where a slight change in δ near this critical value results in a substantial change in the temperature. Several authors have made similar investigations, *e.g.* in [12], [15], [16] and elsewhere. The numerical investigation above calls for further investigations into the effect of the parameter μ and its critical value(s).

In Figure 4, we show the steady-state temperature in the center of each of the subintervals $[0, x_0]$, $[x_0, x_0 + \varepsilon]$ and $[x_0 + \varepsilon, 1]$ as a function of the position x_0 where $\mu_1 = \mu_3 = 1$, $\mu_2 = 10^{-2}$. A similar computation is carried out in Figure 5, but now for $\mu_2 = 10^{-3}$. Comparing these figures, for any position x_0, there is a jump in temperature from the values computed for

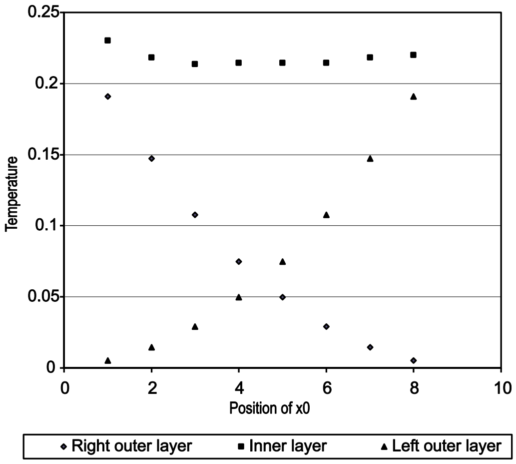

Figure 4. The steady-state temperature in the middle of each of the subintervals $[0, x_0]$, $[x_0, x_0 + \varepsilon]$ and $[x_0 + \varepsilon, 1]$ as a function of the position x_0, where $\mu_1 = \mu_3 = 1$, $\mu_2 = 10^{-2}$ and $\gamma = 0{\cdot}1$.

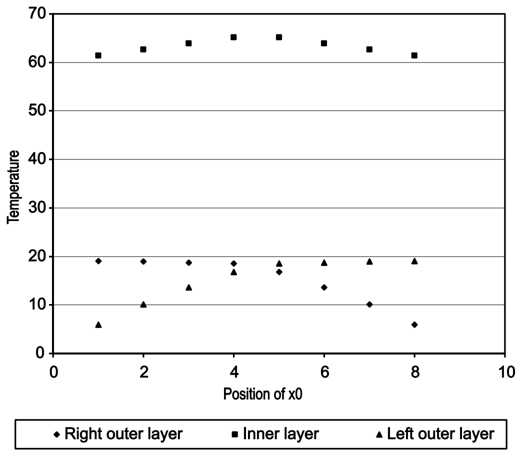

Figure 5. Same as in Figure 4, but now for $\mu_1 = \mu_3 = 1$, $\mu_2 = 10^{-3}$. Notice the temperature jump from the values computed for $\mu_2 = 10^{-2}$ in Figure 4 and those for $\mu_2 = 10^{-3}$ in Figure 5.

$\mu_2 = 10^{-2}$ in Figure 4 to those for $\mu_2 = 10^{-3}$ in Figure 5. These jumps, again, suggest the existence of critical value(s) of μ.

6. Concluding remarks

We have considered a simplified model of the microwave heating of a one-dimensional unit slab. We have described an eigenfunction expansion for the problem based on the Galerkin method and have used a fundamental-mode approximation. We have made an investigation of the bifurcation diagram of the temperature θ *vs*. the parameter δ, where this δ measures the magnitude (power) of the square amplitude of the electric field. The thermal runaway has been investigated through an *S*-shaped curve of an Arrhenius-type reaction rate of the microwave-energy absorption *vs*. temperature. Critical values δ_{cr} and δ^{cr} have been found. The critical value δ^{cr} is of the interest, where slight changes in δ near this critical value result in substantial changes in the temperature. Similar investigations and results can be found in [12, 15, 16] and elsewhere.

We have further applied the approximation to a unit slab consisting of three layers of material with different thermal conductivities. We have taken the thermal conductivity to be of the form $k(\theta) = \mu\, e^{\gamma\theta}$, where θ is the temperature, while the parameter μ has different values in each of the three layers. This μ measures the magnitude of the thermal conductivity of the material. We have addressed the hot-spot formation by finding the global steady-state solution for the whole domain of different thermal conductivities in which the inner layer has a smaller value of the parameter μ.

By making μ smaller in the inner layer than in the outer layers, according to prediction, we find a temperature in this region that is higher than in the rest. The larger the difference of μ in the inner and outer layers, the larger will be the discrepancy of the temperature between the inner layer and the rest of the region. It is very interesting to see that, given a fixed value of δ, there is a jump of the temperature of the inner layer near some value of μ. This jump shows that there is a critical value of the parameter μ below which thermal runaway is experienced, thus signifying the formation of a hot-spot.

We remark that, although the paper is concerned with hot-spot formation, the approach may be applied to a three-layer configuration of a finite slab. Further, the use of Dirichlet boundary conditions, which is very idealistic, allows a more managable investigation into the parameter dependence of the problem. Future work will include more realistic heat-flux conditions on the boundaries and further study on the effects of the parameter μ and its critical value(s) will be done.

Acknowledgments

This research was initiated during a research workshop at Pusat Matematika (P4M-ITB) in August/September 1996 in cooperation with the University of Twente, The Netherlands. Funding for this research was partly provided by the Center Grant (P4M-ITB) and the Royal Netherlands Academy of Arts and Sciences, KNAW. The authors are very grateful to Prof. K. K. Tam, Dr. Edy Soewono, Prof. E. van Groesen and Mr. Toto Nusantara for discussions, suggestions, and encouragement during the writing of this paper. They would like to thank the referees whose comments led to a significant change and expanded version of the original manuscript.

References

1. G. A. Kriegsmann, M. E. Brodwin, D. G. Watter, Microwave heating of ceramic half-space. *SIAM J. Appl. Math.* 50 (1990) 1088–1098.
2. M. E. Brodwin, D. L. Johnson, Microwave sintering of ceramics. *MIT-S* K5 (1988) 287–288.
3. Y. L. Tian, M. E. Brodwin, D. L. Johnson, Ultra-fine microstructure of Al_2O_3 produced by microwave sintering. *Ceramic Trans.* 1 (1987) 925–931.
4. J. C. Araneta, M. E. Brodwin, G. A. Kriegsmann, High temperature characterization of dielectric rods. *IEEE MTT* 32 (1984) 1328–1334.
5. A. J. Bertran, J. C. Badot, High temperature microwave heating in refractory materials. *J. Microwave Power* 11 (1976) 315–320.
6. T. R. Marchant, Microwave heating of materials with impurities. *J. Engng. Math.* 28 (1994) 379–400.
7. G. A. Kriegsmann, Thermal runaway in microwave heated ceramics: A one-dimensional model. *J. Appl. Phys.* 71 (1992) 1960–1966.
8. A. H. Picombe, N. F. Smyth, Microwave heating of materials with low conductivity. *Proc. R. Soc. London A* 433 (1991) 479–498.
9. N. F. Smyth, Microwave heating of bodies with temperature dependent properties. *Wave Motion* 12 (1990) 171–186.
10. T. R. Marchant, A. H. Picombe, Microwave heating of materials with temperature dependent properties. *Wave Motion* 19 (1994) 67–81.
11. C. J. Coleman, On the microwave hot-spot problem. *J. Autral. Math. Soc. Ser. B* 33 (1991) 171–186.
12. J. M. Hill, N. F. Smyth, On the mathematical analysis of hotspots arising from microwave heating. *Math. Engng. Ind.* 2 (1990) 267–278.
13. G. Roussy, A. Bennani, J. Thiebaut, Temperature runaway of microwave irradiated materials. *J. Appl. Phys.* 62 (1987) 1167–1170.
14. J. M. Hill, M. J. Jennings, Formulation of model equations for heating by microwave radiation. *Appl. Math. Mod.* 17 (1993) 1823–1834.
15. J. A. Palesko, G. A. Kriegsmann, Microwave heating of ceramic laminates. *J. Engng. Math.* 32 (1997) 1–18.
16. T. R. Marchant, B. Liu, The steady-state microwave heating of slabs with small Arrhenius absorptivity. *J. Engng. Math.* 33 (1998) 219–236.

17. N. F. Smyth, The effect of conductivity on hotspots. *J. Austral. Math. Soc. Ser. B* 33 (1992) 403–413.
18. Andonowati, *A Study of Some Problems Arising from Combustion and the Microwave Heating.* Ph.D. thesis, Montreal, Canada: McGill University (1995) 102 pp.
19. K. K. Tam, Andonowati, M. T. Kiang, Nonlinear eigenfunction expansion for a problem in microwave heating. *Canad. Appl. Math. Q.* 4 (1996) 311–325.
20. Andonowati, Microwave heating: Critical dependence on data and parameters. In: E. van Groesen and E. Soewono (eds), *Differential Equations: Theory, Numeric, and Applications*. Dordrecht: Kluwer (1997) pp. 189–210.
21. D. A. Frank-Kamenetskii, J. P. Appleton, *Diffusion and Heat Transfer in Chemical Kinetics.* New York: Plenum (1969), 574 pp.
22. A. Lacey, G. C. Wake, Thermal ignition with variable thermal conductivity. *IMA J. Appl. Math.* 28 (1982) 23–39.
23. Andonowati, A two-sided shooting method in computation of travelling combustion waves of a solid material. *J. Austral. Math. Soc. Ser. B.* 38 (1996) 220–228.
24. K. K. Tam, Criticality dependence on data and parameters for a problem in combustion theory, with temperature-dependent conductivity. *J. Austral. Math. Soc. B.* 31 (1989) 76–80.
25. N. Oezisik, *Heat Conduction*. New York: Wiley Interscience (1980), 687 pp.